

Cite this: DOI: 10.1039/xxxxxxxxxx

Photostability of Oxazoline RNA-precursors in UV-rich Prebiotic Environments[†]

 Mikołaj J. Janicki,^a Samuel J. Roberts,^b Jiří Šponer,^c Matthew W. Powner,^{*b} Robert W. Góra,^{*a} and Rafał Szabla,^{*c,d}

Received Date

Accepted Date

DOI: 10.1039/xxxxxxxxxx

www.rsc.org/journalname

Pentose aminooxazolines and oxazolidinone thiones are considered as the key precursors which could have enabled the formation RNA nucleotides under the conditions of early Earth. UV-irradiation experiments and quantum-chemical calculations demonstrate that these compounds are remarkably photostable and could accumulate over long periods of time in UV-rich prebiotic environments to undergo stereoisomeric purification.

Identifying efficient and high-yielding reaction routes towards RNA nucleotides under the conditions of early Earth has been one of the biggest challenges for prebiotic chemistry. Early attempts aiming for the direct formation of the N-glycosidic bond between ribose and nucleobases resulted in either very low reaction yields for purines or virtually no desired products in the case of pyrimidines.¹ While several developments towards a purine pathway have been published recently,² they all remain problematic, for instance requiring the determination of selective and prebiotic sources of pure D-ribose which would prevent the generation of plethora of biologically irrelevant nucleoside analogues. The most efficient alternative reaction routes bypass the glycosylation step by furnishing intermediates, which contain a preformed N-glycosidic bond before the final formation of the de-

sired set of biologically relevant nucleosides.^{3,4} These intermediates, namely ribose (RAO, Fig. 14 in the ESI) and arabinose aminooxazolines (AAO, Fig. 1), constitute an entire sugar moiety, with complete furanosyl selectivity tethered to a nucleobase fragment which efficiently yields ribocytidine and ribouridine in a reaction with cyanoacetylene followed by phosphorylation and UV-irradiation.⁵ While an analogous indirect pathway towards canonical purine ribonucleosides is yet to be demonstrated, a modification of the AAO pyrimidine pathway with sulfur chemistry has enabled the divergent synthesis of pyrimidine and 8-oxo-purine ribonucleotides.⁶ In this case, the role of the intermediate with the preformed N-glycosidic bond was played by arabinose oxazolidinone thione (AOT, Fig. 1).⁶

UV light played a key role in the prebiotically plausible syntheses of RNA monomers. In particular, it promoted efficient cytidine to uridine conversion,⁵ α -2-thiocytidine to β -2-thiocytidine photoanomerisation⁷ and purification of the product mixture from non-biological nucleotide isomers.⁵ However, UV irradiation was considered only for selected steps of these reaction sequences and a more complete understanding of its effects on all the other stages is necessary to ascertain their prebiotic plausibility.

Ranjan and Sasselov scrutinized the characteristics of potential UV environments relevant for the surficial chemistry of early Earth.⁸ First of all, they demonstrated that atmospheric water and CO₂ would efficiently shield wavelengths below 168 nm and 204 nm, respectively. On the other hand, the absence of oxygen in the atmosphere permitted high UV fluxes to reach the surface of prebiotic Earth within the 200 nm to 300 nm spectral window. Consequently, UV-C is likely to have been a major source of energy for prebiotic reactions.⁹ Furthermore, the eradication of the least UV-resistant organic compounds might also play an important role in the prebiotic selection of canonical metabolites.^{3,5}

Our working hypothesis is that the most important intermediates considered in the above reaction sequences should be characterized by high photostability in prebiotically credible UV environments.¹⁰ This feature would be particularly important for the

^a Department of Physical and Quantum Chemistry, Wrocław University of Science and Technology, Faculty of Chemistry, Wybrzeże Wyspiańskiego 27, 50-370, Wrocław, Poland; E-mail: robert.gora@pwr.edu.pl

^b Department of Chemistry, University College London, 20 Gordon Street, London, WC1H 0AJ, UK; E-mail: matthew.powner@ucl.ac.uk

^c Institute of Biophysics of the Czech Academy of Sciences, Královopolská 135, 61265 Brno, Czech Republic; E-mail: szabla@ibp.cz

^d Institute of Physics, Polish Academy of Sciences, Al. Lotników 32/46, 02-668 Warsaw, Poland

[†] Electronic Supplementary Information (ESI) available: [Computational and experimental procedures including methodology, results of irradiation experiments, the corresponding NMR and UV/Vis spectra, compound synthesis and characterization, conformational analysis, characteristics of excited-state stationary points and explicit solvation effects on the excited electronic states]. See DOI: 10.1039/b000000x/

oxazolidinone thione (OT) and aminooxazoline (AO) derivatives, which are synthesized in four different stereoisomeric forms and the enrichment of the relevant stereoisomers could be attained through long-term accumulation and crystallization.^{3,11} Consequently, we focus on discussing the UV-absorption features and radiationless photodeactivation mechanisms of arabinose aminooxazoline (AAO) and arabinose oxazolidinone thione (AOT), which participated in the reaction pathways leading to biologically relevant forms of pyrimidine and 8-oxo-purine nucleosides. For this purpose we used the algebraic diagrammatic construction to the second order [ADC(2)]¹² and CASPT2 methods.¹³ We further validated our theoretical predictions by means of UV-irradiation experiments, which eventually confirmed that these crucial prebiotic intermediates are remarkably photostable.

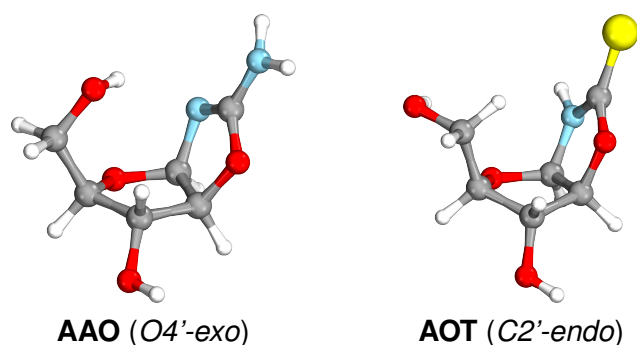


Fig. 1 Ground-state geometries of the most stable conformers of arabinose aminooxazoline (AAO) and arabinose oxazolidinone thione (AOT).

Similar to nucleosides, pentose oxazolines may adopt different conformational arrangements of the sugar ring, albeit more restricted by the *cis*-fused bicyclic C1'-C2' stereocentres. Our ground-state geometry optimizations and ΔG values calculated at the B3LYP-D3/def2-TZVPP level indicate that the O4'-*exo* conformer of AAO and the C2'-*endo* conformer of AOT are likely the most stable forms of these compounds in bulk water (see Fig. 1). We also considered the minimum-energy geometries of alternative C3'-*endo* conformers of AAO and AOT and their ribose stereoisomers (RAO and ROT) which are discussed in the Electronic Supplementary Information (ESI).

Calculations of vertical excitation energies for AAO reveal that the lowest lying optically bright state is a S_2 ($\pi\pi^*$) transition having the excitation energy of 7.02 eV (176 nm), which indicates that the molecule should have little overall absorption at wavelengths longer than 200 nm (see Tab. S1 in the ESI). As observed for thionucleobases,¹⁴ presence of the thiocarbonyl group in AOT results in significant redshift of the UV-absorption spectrum when compared to AAO. The optically bright electronic transition of AOT associated with the π_S and π^* molecular orbitals is located on the thiocarbonyl group and has a noticeably lower excitation energy of 5.32 eV. The lowest-energy singlet state of AOT, lying at 4.06 eV, is also centered around the thiocarbonyl group and can be clearly defined as the $n_S\pi^*$ transition with negligible oscillator strength. It is worth noting that the vertical excitation energies of the above discussed bright $\pi\pi^*$ states in both AAO and AOT are nearly not affected by solvation effects (cf. Tab. S1,

results in parentheses).

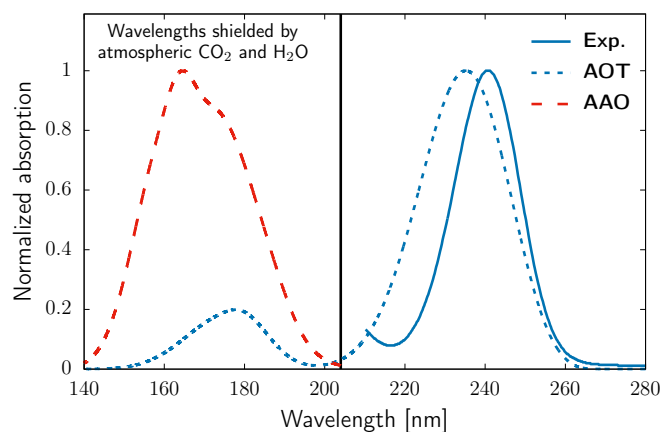


Fig. 2 UV absorption spectra of AAO and AOT simulated with the ADC(2)/cc-pVTZ method and the IMDHO model. Solid curve shows experimental measurements for AOT.

We further performed simulations of UV-absorption spectra at the ADC(2)/cc-pVTZ level within the independent mode displaced harmonic oscillator (IMDHO) approximation in order to estimate the band shapes, using the QM/MM approach to model solvation effects and the resulting inhomogeneous line broadening (see Fig. 2).¹⁵ Consistently with the calculated vertical excitation energies, AAO exhibits negligible absorption at wavelengths longer than 204 nm. The estimated UV-absorption maximum of this compound is located at approximately 165 nm which leaves the predominant part of the spectrum far beyond the typical prebiotic UV fluxes estimated by Ranjan and Sasselov.⁸ While some of the radiationless photodeactivation pathways of AAO were already proposed by Ai *et al.*,¹⁶ we anticipate that this compound would be characterized by high photostability in the environment of early Earth due to its very limited (near-zero) absorption of the available UV light rather than the existence of barrierless nonradiative deactivation mechanisms.

In contrast, the calculated lower-energy absorption maximum of AOT lies at 235 nm, and the molecule exhibits considerable absorption at 250 nm. The simulated UV spectrum is also in very good agreement with our experimental measurements performed in water (cf. Fig. 2). Even though the theoretically predicted absorption maximum is slightly blue-shifted (by 5 nm), the simulation accurately reproduced the onset of UV absorption of AOT. This provides additional confirmation that our computational approach should correctly predict the UV absorption ranges for AAO, for which we cannot measure the experimental spectrum owing to the overlap with the absorption of liquid water.

Apart from CO₂ and H₂O, UV-light could be also partly shielded owing to local releases of SO₂ or H₂S, coming from volcanogenic input, which are much stronger absorbers than CO₂, particularly for wavelengths above 200 nm.⁸ This, however, should be relevant only to periods of high volcanic activity. Although the presence of such sulphur containing gases might be crucial for the formation of compounds like OTs, they are expected to only transiently reach high concentrations in the atmosphere, owing to

their tendencies to be photolyzed or integrated into rock materials. We expect **AOT** to efficiently absorb UV light in such prebiotic environment and we further discuss the photochemical properties and radiationless deactivation mechanisms of this compound.

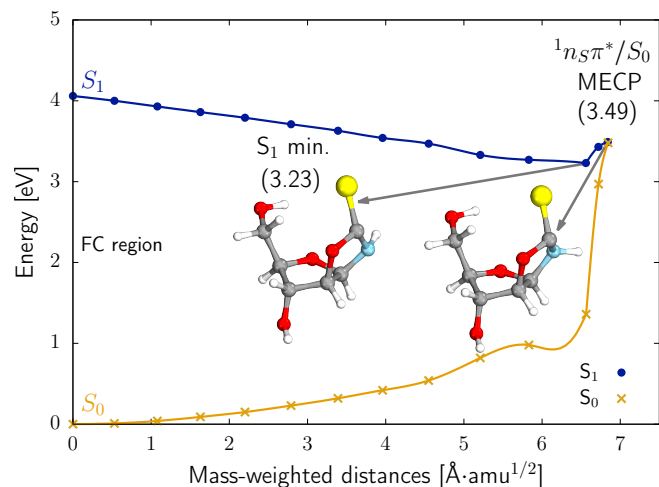


Fig. 3 Potential energy profile showing the singlet photorelaxation mechanism of **AOT** obtained by linear interpolation in internal coordinates (LIIC) between the **AOT** ground-state structure, the S_1 minimum and the S_1/S_0 MECP. The energies of the S_1 and S_0 states were calculated at the ADC(2)/cc-pVTZ and MP2/cc-pVTZ levels, respectively.

Following the UV excitation to the $S_2(\pi_S\pi^*)$ state, **AOT** may further undergo vibrational relaxation towards the minimum on the S_2 hypersurface which is associated with the elongation of the C=S bond and pyramidalization of the thiocarbonyl carbon atom. The vertical energy difference between the S_2 and S_1 states, computed at the S_2 minimum-energy geometry, amounts to 0.43 eV, which indicates that the relaxation to the lowest-lying singlet state might be delayed by a modest energy barrier. The S_2/S_1 minimum energy crossing point (MECP) enabling a radiationless transition to the lowest-lying singlet state is of slightly sloped topography and is 0.36 eV higher in energy than the S_2 minimum. This suggests that UV-excited **AOT** could linger in the bright $S_2(\pi_S\pi^*)$ state for several tens of fs before reaching the S_2/S_1 MECP. However, considering the excess energy gained by the molecule during UV excitation above 5.0 eV, we expect the population of the dark $S_1(n_S\pi^*)$ to be quite efficient.

The subsequent radiationless photodeactivation mechanism of **AOT** available in the dark $S_1(n_S\pi^*)$ state is presented in Fig. 3. Similar to the S_2 minimum, the S_1 minimum-energy geometry is characterized by the elongated C-S bond (1.77Å compared to 1.63Å in the ground-state geometry), and pyramidalized thiocarbonyl carbon atom. Further tilting of the thiocarbonyl group, more pronounced pyramidalization of the corresponding carbon atom and additional umbrella-like flipping of the N-H bond may drive the molecule towards the sloped $S_1(n_S\pi^*)/S_0$ conical intersection, lying 0.27 eV above and only 0.28 Å·amu^{1/2} from the S_1 minimum. This energy difference was also confirmed by additional CASPT2 calculations (0.28 eV; cf. the ESI) and is low enough to enable prompt photorelaxation to the electronic ground state, owing to the high energy of UV photons absorbed

by **AOT**. Consequently, we anticipate that this photodeactivation channel should be very efficient.

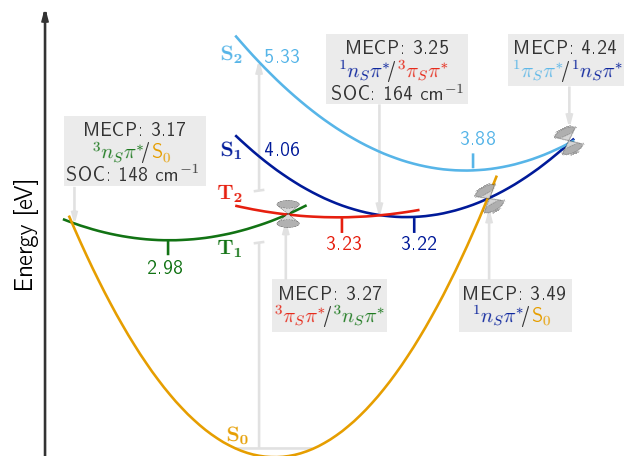


Fig. 4 Schematic representation of the photorelaxation pathways available for **AOT**. Energies of all the presented stationary points were computed at the ADC(2)/cc-pVTZ level of theory.

Recent studies of the photochemistry of thionated nucleobases and nucleosides revealed that this simple structural modification results in near-unity triplet yields and significant enhancement of reactive photochemistry occurring in the triplet manifold of electronic states.¹⁴ Our calculations of spin-orbit coupling (SOC) matrix elements at optimized MECPs demonstrate that singlet-triplet intersystem crossing (ISC) rates in **AOT** may be comparably high (cf. Fig. 4). In particular, the S_1/T_2 MECP corresponds to the El-Sayed allowed $^1n_S\pi^* \rightsquigarrow ^3\pi_S\pi^*$ ISC and is nearly isoenergetic with the above discussed $S_1(^1n_S\pi^*)$ minimum. The associated SOC amounts to 164 cm⁻¹ which further confirms the importance of the S_1/T_2 MECP. The ISC rate constant estimated using the Condon approximation to the Fermi's golden rule,¹⁷ is relatively high and amounts to $1.11 \cdot 10^{11} \text{ s}^{-1}$. This indicates that the $^1n_S\pi^* \rightsquigarrow ^3\pi_S\pi^*$ ISC could operate on a picosecond timescale and efficiently compete with the singlet photorelaxation pathway.

The T_2/T_1 conical intersection enables further relaxation of **AOT** after the population of the triplet $^3\pi_S\pi^*$ state. The optimized T_2/T_1 MECP is also nearly isoenergetic with the S_1 minimum, which implies that the cascade of transitions driving UV-excited **AOT** to the lowest-energy triplet state could be very efficient. In opposition to thionucleobases which triplet photochemistry is generally dominated by $^3\pi\pi^*$ excitations,¹⁴ the T_1 state of **AOT** is of pure $^3n_S\pi^*$ character. This entails intriguing implications for its anticipated photoreactivity. First of all, we expect the triplet and singlet photochemistry of **AOT** to be very similar, particularly since the structural deformations related to both S_1 and T_1 states are virtually identical. In addition, the photodeactivation through the T_1/S_0 MECP should also be fairly rapid owing to high SOC of 148 cm⁻¹ between the involved T_1 and S_0 electronic states. Since we were unable to locate any other T_1 minimum which could be potentially associated with a different electronic transition (e.g. $^3\pi\pi^*$), we expect this channel to be the dominant contributor to the triplet photorelaxation of UV-excited **AOT**. It is worth not-

ing that the $T_1(^3n_s\pi^*)$ minimum can be additionally stabilized in aqueous environments by an interaction between the n orbital of the thiocarbonyl group and the p_z orbital of a neighbouring water molecule (see the ESI for more details).

To validate our theoretical prediction of highly efficient photodeactivation mechanisms and short-lived excited electronic states which would significantly impede photodestructive bimolecular reactions of **AOT**, we performed UV-irradiation experiments of aqueous **AOT** and ribose oxazolidinone thione (**ROT**). Following a 16 h UV-irradiation (254 nm principle emission) of **AOT** and **ROT**, thiones were recovered in 68% and 47%, respectively, alongside a small amount of photo-hydrolysis to their respective arabinose and ribose oxazolidinones (4% and 10%). Analogous UV-irradiation of thiones **AOT** and **ROT** at 300 nm for 16 h proved significantly less destructive and we recovered 83% of **AOT** and 78% **ROT**. This is a result of the apparent transparency of **AOT** and **ROT** to UV light at 300 nm. In addition, we observed no photo-hydrolysis at this wave-length. Given that the photoflux and likely duration of irradiation on the early Earth cannot be quantified, we decided it was appropriate to compare the UV-resistance of thiones **AOT** and **ROT** to compounds of known photostability to provide a quantifiable relative assessment of their photostability in UV-rich prebiotic environments. Adenine and adenosine are among the most photostable biomolecular building blocks and therefore we chose them for such direct comparisons.^{18,19} Simultaneous UV-irradiation of **AOT** with adenine at 254 nm returned these starting materials in 80% and 100%, respectively, together with the product of photo-hydrolysis, i.e. oxazolidinone in 3% yield, after 16 h. A comparable irradiation (at 254 nm) of **AOT** with adenosine returned 79% and 82% of these starting materials, respectively, alongside small amounts of oxazolidinone (9%). These results clearly demonstrate that the photostability of oxazolidinone thiones is directly comparable to that of purine ribonucleotides.

In summary, we have shown that both arabinose amino-oxazoline (**AAO**) and oxazolidinone thione (**AOT**) are resistant to persistent UV irradiation in prebiotically credible environment of early Earth. In particular we emphasize here, that apart from exploration of photorelaxation pathways, it is important to consider whether prebiotic molecules absorb within the spectrum of UV-light that was likely to be delivered to the surface of early Earth. **AAO** was observed to be a photostable prebiotic precursor of RNA nucleotides owing to its negligible absorption of UV light above 200 nm. The same would apply to **AOT** during periods of high volcanic activity, when the spectral range between 200–300 nm would be transiently screened by atmospheric SO_2 and H_2S . **AOT** efficiently absorbs UV-light which is expected to have reached the surface of primordial Earth in the absence of these gases. However, our irradiation experiments indicate that this compound is photostable and undergoes fast nonradiative deactivation. The results of ab initio calculations indicate that this is due to efficient internal conversion in the singlet manifold which could be accompanied by smooth intersystem crossing to the triplet manifold of electronic states. Although triplet excitations are generally regarded as reactive channels in organic photochemistry, very high SOC between $T_1(^3n_s\pi^*)$ and S_0 states should enable **AOT** to ef-

ficiently repopulate the closed-shell singlet ground state and protect it from destructive bimolecular radical reactions. In addition, preliminary calculations and experiments performed for ribose amino-oxazoline (**RAO**) and ribose oxazolidinone thione (**ROT**) demonstrate generally similar photochemical and photophysical properties to their arabinose isomers. Based on these findings, we expect that the oxazoline RNA-precursors could accumulate over long periods of time under persistent UV irradiation allowing stereoisomeric purification via crystallization.^{3,5,11} These results further reinforce the prebiotic plausibility of the synthetic pathways to RNA nucleotides involving oxazoline intermediates and constituting photochemical reaction steps.^{5–7}

This work was supported in part by the Simons Foundation (318881 to M.W.P., 494188 to R.S.), and a grant from the National Science Centre Poland (2016/23/B/ST4/01048 to R.W.G.). Statutory activity subsidy from the Polish Ministry of Science and Higher Education for the Faculty of Chemistry of Wrocław University of Science and Technology is gratefully acknowledged. M.J.J. acknowledges support within the “Diamond Grant” (0144/DIA/2017/46) from the Polish Ministry of Science and Higher Education.

References

- (a) L. E. Orgel, *Crit. Rev. Biochem. Mol. Biol.*, 2004, **39**, 99–123; (b) J. D. Sutherland, *Angew. Chem. Int. Ed.*, 2016, **55**, 104–121.
- (a) S. Becker, I. Thoma, A. Deutsch, T. Gehrke, P. Mayer, H. Zipse and T. Carell, *Science*, 2016, **352**, 833–836; (b) H.-J. Kim and S. A. Benner, *Proc. Natl. Acad. Sci. U.S.A.*, 2017, **114**, 11315–11320; (c) M. W. Powner, J. D. Sutherland and J. W. Szostak, *J. Am. Chem. Soc.*, 2010, **132**, 16677–16688; (d) W. D. Fuller, R. A. Sanchez and L. E. Orgel, *J. Mol. Biol.*, 1972, **67**, 25–33.
- S. Islam, D.-K. Bučar and M. W. Powner, *Nat. Chem.*, 2017, **9**, 584–589.
- S. Islam and M. W. Powner, *Chem*, 2017, **2**, 470–501.
- (a) M. W. Powner, B. Gerland and J. D. Sutherland, *Nature*, 2009, **459**, 239–242; (b) G. Springsteen and G. F. Joyce, *J. Am. Chem. Soc.*, 2004, **126**, 9578–9583; (c) C. Anastasi, M. A. Crowe, M. W. Powner and J. D. Sutherland, *Angew. Chem. Int. Ed.*, 2006, **45**, 6176–6179; (d) M. Powner and J. Sutherland, *ChemBioChem*, 2008, **9**, 2386–2387.
- S. Stairs, A. Nikmal, D.-K. Bučar, S.-L. Zheng, J. W. Szostak and M. W. Powner, *Nat. Commun.*, 2017, **8**, 15270.
- J. Xu, M. Tsanakopoulou, C. J. Magnani, R. Szabla, J. E. Šponer, J. Šponer, R. W. Góra and J. D. Sutherland, *Nat. Chem.*, 2017, **9**, 303–309.
- (a) S. Ranjan and D. D. Sasselov, *Astrobiology*, 2017, **17**, 169–204; (b) S. Ranjan and D. D. Sasselov, *Astrobiology*, 2016, **16**, 68–88.
- R. J. Rapf and V. Vaida, *Phys. Chem. Chem. Phys.*, 2016, **18**, 20067–20084.
- (a) R. Szabla, D. Tuna, R. W. Góra, J. Šponer, A. L. Sobolewski and W. Domcke, *J. Phys. Chem. Lett.*, 2013, **4**, 2785–2788; (b) R. Szabla, J. E. Šponer, J. Šponer, A. L. Sobolewski and R. W. Góra, *Phys. Chem. Chem. Phys.*, 2014, **16**, 17617–17626; (c) R. Szabla, J. Šponer and R. W. Góra, *J. Phys. Chem. Lett.*, 2015, **6**, 1467–1471.
- J. E. Hein, E. Tse and D. G. Blackmond, *Nat. Chem.*, 2011, **3**, 704–706.
- (a) C. Hättig, *Advances in Quantum Chemistry*, Academic Press, 2005, vol. 50, pp. 37–60; (b) A. Dreuw and M. Wormit, *Wiley Interdiscip. Rev. Comput. Mol. Sci.*, 2015, **5**, 82–95.
- (a) J. Finley, P.-A. Malmqvist, B. O. Roos and L. Serrano-Andrés, *Chem. Phys. Lett.*, 1998, **288**, 299–306; (b) T. Shiozaki, W. Györfy, P. Celani and H.-J. Werner, *J. Chem. Phys.*, 2011, **135**, 081106.
- (a) L. Martínez-Fernández, I. Corral, G. Granucci and M. Persico, *Chem. Sci.*, 2014, **5**, 1336–1347; (b) S. Mai, M. Pollum, L. Martínez-Fernández, N. Dunn, P. Marquetand, I. Corral, C. E. Crespo-Hernández and L. González, *Nat. Commun.*, 2016, **7**, 13077; (c) S. Mai, P. Marquetand and L. González, *J. Phys. Chem. Lett.*, 2016, **7**, 1978–1983; (d) M. J. Janicki, R. Szabla, J. Šponer and R. W. Góra, *Chem. Phys.*, 2018.
- (a) T. Petrenko and F. Neese, *J. Chem. Phys.*, 2012, **137**, 234107; (b) R. Zalesny, N. A. Murugan, F. Gel'mukhanov, Z. Rinkevicius, B. Ośmiatowski, W. Bartkowiak and H. Ågren, *J. Phys. Chem. A*, 2015, **119**, 5145–5152.
- Y. Ai, S. Xia and R.-Z. Liao, *J. Phys. Chem. B*, 2016, **120**, 9329–9337.
- M. Etinski, J. Tatchen and C. M. Marian, *J. Chem. Phys.*, 2011, **134**, 154105.
- S. Boldissar and M. S. d. Vries, *Phys. Chem. Chem. Phys.*, 2018, **20**, 9701–9716.
- D. Tuna, A. L. Sobolewski and W. Domcke, *J. Phys. Chem. A*, 2014, **118**, 122–127.